O-Glycosylation of Axl2/Bud10p by Pmt4p Is Required for Its Stability, Localization, and Function in Daughter Cells

Sylvia L. Sanders,* Martina Gentzsch,‡ Widmar Tanner,‡ and Ira Herskowitz*

*Department of Biochemistry and Biophysics, University of California, San Francisco, California 94143-0448; and ‡Lehrstuhl für Zellbiologie und Pflanzenphysiologie, Universität Regensburg, D-93053 Regensburg, Germany

Abstract. Cells of the yeast *Saccharomyces cerevisiae* choose bud sites in a manner that is dependent upon cell type: **a** and α cells select axial sites; **a**/α cells utilize bipolar sites. Mutants specifically defective in axial budding were isolated from an α strain using pseudohyphal growth as an assay. We found that **a** and α mutants defective in the previously identified *PMT4* gene exhibit unipolar, rather than axial budding: mother cells choose axial bud sites, but daughter cells do not. *PMT4* encodes a protein mannosyl transferase (pmt) required for O-linked glycosylation of some secretory and cell surface proteins (Immervoll, T., M. Gentzsch, and W. Tanner. 1995. *Yeast*. 11:1345–1351). We demonstrate that Axl2/Bud10p, which is required for the axial budding pattern, is an O-linked glycoprotein and is incompletely glycosylated, unstable, and mislocalized in cells lacking *PMT4*. Overexpression of *AXL2* can partially restore proper bud-site selection to *pmt4* mutants. These data indicate that Axl2/Bud10p is glycosylated by Pmt4p and that O-linked glycosylation increases Axl2/Bud10p activity in daughter cells, apparently by enhancing its stability and promoting its localization to the plasma membrane.

Key words: O-glycosylation • *PMT4* • *AXL2/BUD10* • budding • polarity

YEAST cells grow by budding, a specialized form of cell division. Bud emergence occurs in the G1 phase of the cell cycle at predictable locations on the cell surface. Several proteins required for bud emergence, including actin and the rho-type GTPase, Cdc42p (Adams and Pringle, 1984; Ziman et al., 1993), assemble at this site. Subsequently, the actin cytoskeleton is polarized towards this site, which leads to polarized secretion, cell surface growth, and formation of a bud (Tkacz and Lampen, 1973; Field and Schekman, 1980; Adams and Pringle, 1984; Novick and Botstein, 1985). Cytokinesis later occurs at the position of bud emergence, resulting in a mother and a daughter cell. Thus, when cells choose bud sites, they fix the orientation of the actin cytoskeleton, the polarity of secretion, and the position for cytokinesis.

The position of bud assembly is specified by a set of bud-site selection genes and by cell type (Hicks et al., 1977; Bender and Pringle, 1989; Chant and Herskowitz, 1991; Chant et al., 1991; Valtz and Herskowitz, 1996; Zahner et al., 1996). **a** and α cells choose sites in an axial pattern, in which cells bud adjacent to the previous division site. **a**/α cells choose bipolar sites, in which daughter cells (cells that have not budded previously) typically bud distal to the previous division site; mother cells (cells that have budded previously) choose sites proximal or distal to the previous division site (Freifelder, 1960; Chant and Pringle, 1995). The ability of cells to exhibit predictable budding patterns suggests that intracellular landmarks direct the position of bud emergence (Chant and Herskowitz, 1991; Snyder et al., 1991). The behavior of two classes of mutants is consistent with this landmark hypothesis. Mutations in *BUD3*, *BUD4*, *AXL1*, or *AXL2/BUD10* disrupt the axial budding pattern, but have no effect on the bipolar budding pattern of **a**/α cells (Chant and Herskowitz, 1991; Chant et al., 1991; Fujita et al., 1994; Halme et al., 1996; Roemer et al., 1996). In contrast, mutations in *BNI1*, *SPA2*, *PEA2*, *BUD6*, *BUD7*, *BUD8*, or *BUD9* disrupt the bipolar budding pattern, but have no effect on the axial budding pattern of **a** and α cells (Valtz and Herskowitz, 1996; Zahner et al., 1996; Amberg et al., 1997). The first set of genes is specifically required for the axial budding pattern, whereas the second set is specifically required for the bipolar budding pattern.

S.L. Sanders' present address is Department of Biology, Massachusetts Institute of Technology and Howard Hughes Medical Institute, 31 Ames Street, Cambridge, MA 02139.

M. Gentzsch's present address is Mayo Clinic Scottsdale, S.C. Johnson Medical Research Center, 13400 East Shea Boulevard, Scottsdale, AZ 85259.

Address correspondence to Sylvia Sanders, Department of Biology, Massachusetts Institute of Technology and Howard Hughes Medical Institute, 31 Ames Street, Cambridge, MA 02139. Tel.: (617) 258-5152. Fax: (617) 253-6742. E-mail: sylvias@mit.edu

For cells budding in the axial pattern, the bud site used in one cell cycle specifies an adjacent position for bud emergence in the next cell cycle (Chant and Pringle, 1995). Bud3p, Bud4p, and Axl2/Bud10p are located in a cortical position at the mother-bud neck from mitosis of one cell cycle to G1 of the next (Chant et al., 1995; Halme et al., 1996; Roemer et al., 1996; Sanders and Herskowitz, 1996). Thus, during G1, Bud3p, Bud4p, and Axl2/Bud10p behave as spatial remnants of the position of bud emergence in the previous cell cycle and promote adjacent bud emergence in the new cell cycle. These cortical factors are proposed to organize the cytoskeleton by recruiting downstream proteins required for bud emergence, such as Cdc24p and Bem1p, to that site (Sloat and Pringle, 1978; Bender and Pringle, 1991). Indeed, Rsr1p/Bud1p, required for both axial and bipolar budding, binds to bud emergence proteins Cdc24p and Bem1p (Zheng et al., 1995; Park et al., 1997), and Bud6p interacts with actin in the yeast two-hybrid assay (Amberg et al., 1995, 1997).

Axl2/Bud10p is a type I integral membrane protein that is thought to provide spatial information for the axial pattern (Halme et al., 1996; Roemer et al., 1996). It traverses the secretory pathway to reach its final destination at the plasma membrane and contains N-linked oligosaccharides. Axl2/Bud10 has a receptor-like topology: a single transmembrane domain and substantial intra- and extracellular domains. The large NH_2-terminal domain is extracellular, rich in serine and threonine residues, and is postulated to interact with the cell wall. During G1, Axl2/Bud10p is present first at the presumptive bud site and later at the periphery of the bud. As the bud grows, Axl2/Bud10p is found in an apparent ring structure on the bud side of the mother-bud neck. It later forms an additional apparent ring on the mother side of the mother-bud neck during mitosis. Initial localization of Axl2/Bud10p to the neck requires septin proteins (Roemer et al., 1996). Subsequent organization of Axl2/Bud10p into rings at the neck requires Bud3p (Halme et al., 1996).

In the present study, we describe a requirement for O-glycosylation in bud-site selection. Yeast has seven protein mannosyl transferases (pmt)[1], encoded by *PMT* genes, that catalyze the initial step of O-linked glycosylation (Tanner and Lehle, 1987; Gentzsch and Tanner, 1996). These enzymes transfer a mannosyl residue from a dolichol-phosphate donor onto serine or threonine residues of substrate proteins in the endoplasmic reticulum (Haselbeck and Tanner, 1983; Strahl-Bolsinger and Tanner, 1991; Immervoll et al., 1995; Lussier et al., 1995; Gentzsch and Tanner, 1996). Further modification of these O-linked oligosaccharides occurs in the Golgi apparatus (Haselbeck and Tanner, 1983; Herscovics and Orlean, 1993). Pmts are required for cell wall integrity, cell morphology, and coordination of the nuclear and morphological cell cycles (Gentzsch and Tanner, 1996). We show here that mutations in the mannosyl transferase gene *PMT4* affect the axial budding pattern of **a** and α cells. The requirement of Pmt4p for bud-site selection appears to result from its O-linked glycosylation of Axl2/Bud10p.

1. *Abbreviations used in this paper: BAD*, bud-site selection axial determinant; GFP, green fluorescent protein; HA, hemagglutinin epitope; HF, hydrogen fluoride; ORF, open reading frame; pmt, protein mannosyl transferase; PNGase, peptide N-glycosidase F; SLAHD, synthetic low ammonium histidine dextrose; WT, wild-type.

Materials and Methods

Materials

HA11 mAb, used to detect the hemagglutinin epitope (HA) in an Axl2/Bud10p-HA fusion protein, was from Berkeley Antibody Company. Polylysine, protease inhibitors (phenylmethylsulfonyl fluoride, benzamidine, antipain, leupeptin, and pepstatin), calcofluor white, and protein standards were from Sigma Chemical Co. HRP-coupled sheep anti–mouse antibodies were from Nycomed Amersham, Inc. Peptide N-glycosidase F (PNGase) and tunicamycin were from Boehringer Mannheim Corp.

Microbiological and Molecular Biological Methods

Strains are described in Table I, and plasmids in Table II. DNA and yeast genetic manipulations were performed as described (Ausubel et al., 1987; Sambrook et al., 1989; Rose et al., 1990). Synthetic low ammonium histidine dextrose (SLAHD) solid medium for assaying pseudohyphal growth was prepared as described by Gimeno et al. (1992). Microcolony budding assays were performed as previously described (Chant and Herskowitz, 1991; Sanders and Herskowitz, 1996).

Isolation of Axial-defective Mutants

Construction of SY77. The *HMR**a*** gene of IH2531 (α *ura3-52*) was disrupted by introduction of pDR58 digested with EcoRV (Loo et al., 1995), creating SY77. The disruption was confirmed by Southern blot analysis.

Mutagenesis. A culture of SY77 was grown to saturation in rich medium, resuspended in water, and UV-irradiated in separate aliquots to 0.3–24% survival. Mutagenized cells were plated on solid SLAHD medium to induce pseudohyphal growth (Gimeno et al., 1992) and incubated at 30°C for 2 wk in the dark. Of ~70,000 surviving colonies, 407 exhibited the pseudohyphal colony morphology. Microcolony budding assays were performed on the 107 colonies that retested for pseudohyphal growth. 23 of these mutants exhibited >30% bipolar budding and were studied further.

Genetic Tests. Mutants were tested for single-gene segregation by analyzing the budding pattern of the meiotic progeny of crosses to IH2393 (**a** Bud^+). Mutants whose progeny exhibited 2:2 axial/bipolar budding were studied further. Because **a**/α strains do not exhibit the axial budding pattern, dominance or recessiveness was assessed by analyzing *mat**a**1/MAT*α diploid progeny (phenotypically α) formed by crosses between the mutants and a *mat**a**1* strain (IH1785). Recessive mutations yielded an axial budding pattern in the *mat**a**1/MAT*α diploids; dominant or semidominant mutations yielded a bipolar or partially bipolar phenotype. Mutants defective in known genes required for axial budding were identified by complementation tests using plasmids carrying *BUD3*, *BUD4*, or *AXL1*, by mating to *bud3*, *bud4*, *axl1*, or *axl2* strains, and, for new *BUD4* and *AXL1* alleles, by linkage tests. Complementation tests among the mutants were performed by analyzing diploids (phenotypically α) formed by crossing *mat**a**1* and α mutant strains. If the resultant diploid exhibited axial budding, the two mutations were assigned to different complementation groups. If the resultant diploid exhibited bipolar budding, the two mutations were assigned to the same complementation group.

Cloning BAD15/PMT4

The bud-site selection axial determinant *BAD15/PMT4* gene was cloned by complementation of the pseudohyphal growth phenotype. SY167 (α *bad15-1 ura3*) was transformed with a low copy yeast library marked with *URA3* (Rose et al., 1987). Approximately 10,200 transformants were patched onto SLAHD plates in two concentric rings of 25 (because the pseudohyphal phenotype in **a** and α cells was sensitive to position on the plate, as well as the number of colonies per plate). Plates were incubated for 2 wk at 30°C and scored for pseudohyphae by microscopic examination at 30×. Nine transformant colonies failed to exhibit pseudohyphal growth and were assayed for budding pattern. Plasmid DNA isolated from the three colonies that exhibited axial budding contained overlapping inserts by restriction analysis.

Table I. Strains Used in this Study

Strain	Genotype	Source
IH2531	α *ura3-52*	Gimeno et al., 1992
SY96*	α *ura3-52*	Fink Laboratory
SY77*	α *hmr**a***::*URA3*	This study
SY167*	α *bad15 ura3*	This study
SY172*	α *bad43 ura3*	This study
SY171*	α *bud4-3*	This study
SY202	***a***/α *bad15/bad15 ura3/+ his4/+ trp1/+* (isogenic with SY204)	This study
SY204	***a***/α *ura3/+ his4/+ trp1/+* (isogenic with SY202)	This study
MY16*	α *leu2 ura3-52*	M. Maxon, IH Lab
SY448*	α *leu2 pmt4*::*LEU2*	This study
MY13*	***a*** *leu2*	M. Maxon, IH Lab
SY447*	***a*** *leu2 pmt4*::*LEU2*	This study
SY463	***a***/α *leu2/leu2*	This study
SY464	***a***/α *pmt4*::*LEU2/pmt4*::*LEU2 leu2/leu2*	This study
SY414	α *leu2-3 ura3-52 his3-*Δ*200 lys2-801 trp1-*Δ*901 suc2-*Δ*9*	Tanner Lab Collection
SY655‡	α *pmt1*::*URA3*	Tanner Lab Collection
SY656‡	α *pmt2*::*LEU2*	Tanner Lab Collection
SY657‡	α *pmt3*::*HIS3*	Tanner Lab Collection
SY415‡	α *pmt4*::*TRP1*	Tanner Lab Collection
SY658‡	α *pmt5*::*URA3*	Tanner Lab Collection
SY659‡	α *pmt6*::*URA3*	Tanner Lab Collection
IH1783	***a*** *trpl leu2 ura3 his4 can1*	IH Lab Collection
SY450§	***a*** *pmt4*::*LEU2*	This study
SY748§	*mat*::*URA3 pmt4*::*LEU2*	This study
IH1785§	*mat**a**l-50*	IH Lab Collection
SY221	*mat**a**l-50 bad15 his4 leu2 ura3*	This study
MGY60‡	α *axl2*::*AXL2-HA*	This study
MGY61‡	α *pmt1*::*HIS3 axl2*::*AXL2-HA*	This study
MGY62‡	α *pmt2*::*LEU2 axl2*::*AXL2-HA*	This study
MGY63‡	α *pmt3*::*HIS3 axl2*::*AXL2-HA*	This study
MGY64‡	α *pmt4*::*TRP1 axl2*::*AXL2-HA*	This study
MGY65‡	α *pmt5*::*URA3 axl2*::*AXL2-HA*	This study
MGY66‡	α *pmt6*::*LYS2 axl2*::*AXL2-HA*	This study
YWO333	α *ade2-1^o his3-11,15 leu2-3,112 trp1-1 ura3-1 can1-100*	Dieter Wolf
YWO339‖	***a*** *pep4*Δ::*HIS3 prb1*::*LEU2*	Dieter Wolf
YWO340‖	***a*** *pep4*Δ::*HIS3 prb1*::*hisG prc1*::*hisG*	Dieter Wolf
MGY69‖	α *axl2*::*AXL2-HA*	This study
MGY70‖	***a*** *pep4*Δ::*HIS3 prb1*::*LEU2 axl2*::*AXL2-HA*	This study
MGY71‖	***a*** *pep4*Δ::*HIS3 prb1*::*hisG prc1*::*hisG axl2*::*AXL2-HA*	This study
MGY72‖	α *pmt4*Δ::*TRP1 axl2*::*AXL2-HA*	This study
MGY73‖	***a*** *pmt4*::*TRP1 pep4*Δ::*HIS3 prb1*::*LEU2, axl2*::*AXL2-HA*	This study
MGY74‖	***a*** *pmt4*::*TRP1 pep4*::*HIS3 prb1*::*hisG prc1*::*hisG axl2*::*AXL2-HA*	This study
MGY67‡	α *axl2*::*AXL2-HA ubc7*::*LEU2*	This study
MGY68‡	α *pmt4*::*TRP1 axl2*::*AXL2-HA ubc7*::*LEU2*	This study
MGY75¶	*axl2*::*AXL2-HA*	This study
MGY76¶	α *ura3-52 leu2-3,112 suc2-*Δ*9 sec7axl2*::*AXL2-HA pmt4*::*LEU2*	This study
MGY77†	*axl2*::*AXL2-HA*	This study
MGY78†	α *ura3-52 leu2-3,112 suc2-*Δ*9 sec18axl2*::*AXL2-HA pmt4*::*LEU2*	This study

*Isogenic to IH2531, except where noted.
‡Isogenic to SY414, except where noted.
§Isogenic to IH1783, except where noted.
‖Isogenic to YWO333, except where noted.
¶Isogenic to SEY5018, except where noted.
†Isogenic to SEY5188, except where noted.

Complete Deletion of PMT4

The *pmt4*Δ constructs replaced the entire *PMT4* coding sequence with the *LEU2* or *TRP1* gene. The HindIII–SalI fragment of pSS47, which contains *PMT4* and YJR142W, was cloned into the vector pBluescript (Stratagene), creating pSS48. All sequences of pSS48, except the *PMT4* open reading frame (ORF), were amplified using PCR with divergent primers (OSS8 5′-CCGaggcctCTTTTTCTGTTCACTAACCACAAACGAACTG and OSS9 5′-CCGaggcctCTGTACTTCTGTGGACTGTCAGAAAATATCTTGG; a StuI restriction site is denoted in lower case) that hybridized just upstream of the *PMT4* start codon and downstream of the stop codon. The resulting linear fragment was cleaved at the introduced StuI sites and circularized, yielding a plasmid (pSS49) that contained the *PMT4* flanking regions separated by the StuI site. The *LEU2* gene was then introduced into the StuI site to form pSS51, with the direction of *LEU2* transcription opposite that of *PMT4*. The resulting disruption fragment was excised from pSS51 by digestion with HindIII and SphI and used to replace the chromosomal *PMT4* gene by one-step gene replacement (Rothstein, 1983). The presence of the *pmt4* deletion was confirmed by colony PCR with the following oligonucleotides: OSS10, derived from

Table II. Plasmids Used in this Study

Plasmid	Description	Source
pDR58	*hmra*::*URA3* knock-out construct	D. Rivier, University of Illinois
pSS51	*pmt4*::*LEU2* knock-out construct	This study
pSS52	*pmt4*::*TRP1* knock-out construct	This study
pAH14	*AXLBUD10*-GFP in pRS314	Halme et al., 1996
pRS314	CEN ARS vector containing *TRP1*	Sikorski and Hieter, 1989
p*AXL2-HA*	Encodes *AXL2-HA*; inYIp5	Roemer et al., 1996
YEp24-*AXL2*	*2μ AXL2*	Roemer et al., 1996
B1,B5,B7,B9	Original *bad15* complementing clones in YCp50 containing ORFs YJR140C-YJR147W	This study; Rose et al., 1987
pSS44	B7 lacking the ~4.5 kB SphI fragment (one SphI site was from the plasmid vector), contains ORFs YJR140C-YJR143C (*PMT4*)	This study
pSS45	ClaI-HpaI fragment of B7 cloned into the ClaI-NruI sites of Ycp50, contains all of YJR142W and a portion of YJR143C (*PMT4*)	This study
pSS46	EcoRI-BglII fragment of pSS44 in the EcoRI-BamHI sites of YCp50, contains all of YJR140C, YJR141W, and a portion of YJR142W	This study
pSS47	pSS44 lacking the HindIII fragment, contains all of ORFs YJR142W and YFR143C (*PMT4*)	This study
pSS48	HindIII-SalI fragment of pSS47 cloned into the HindIII-SalI sites of pBluescript (Stratagene)	This study
pSS49	pSS48 lacking the *PMT4* ORF (see Materials and Methods)	This study

LEU2: 5′-TTAGACCGCTCGGCCAAACAACC; and OSS11, derived from the *PMT4* 3′ sequences not present in the pSS49 plasmid, 5′-GGCCATACCATGAAGTATACC; amplified a ~0.8-kB fragment in *pmt4*::*LEU2* cells. Control oligonucleotides: OSS7, derived from the *PMT4* 3′ flanking sequences, 5′-CCGAGGCCTCTGTACTTCTGTGGACTGTCAGAAAATATCTTGG; and OSS11 amplified a ~0.5-kB fragment in Pmt^+ cells. To create a *pmt4*::*TRP1* allele, the HincII–StuI fragment of YPP14, containing *TRP1*, was introduced into the StuI site of pSS49. The resultant plasmid, pSS52, was digested with ClaI and SphI and used to disrupt the chromosomal copy of *PMT4* by one-step gene replacement (Rothstein, 1983). The presence of the *pmt4* deletion was confirmed by analyzing bud-site selection pattern.

Membrane Extracts and Western Blot Analysis

Yeast cells grown overnight and harvested in log phase were washed with 50 mM Tris-HCl, pH 7.5, 50 mM $MgCl_2$, 1 mM phenylmethylsulfonyl fluoride, 1 mM benzamidine, and disrupted with glass beads in the same buffer containing 20 μg/ml antipain, 1 μg/ml leupeptin, and 1 μg/ml pepstatin. The cell wall fraction was removed by centrifugation at 1,500 *g*. The resulting supernatant was centrifuged at 48,000 *g* to generate a membrane pellet. 5 to 10 μg of membrane protein was subjected to SDS-PAGE using 8 or 10% SDS-polyacrylamide gels. Proteins were transferred to nitrocellulose membranes, blocked in TBS containing 0.1% Tween 20 and 4% nonfat dry milk, and decorated with a 1:1,000 dilution of HA antibodies in TBS containing 0.1% Tween 20 and 1% nonfat dry milk. Axl2/Bud10p-HA was visualized using the Nycomed Amersham ECL protein detection kit.

Peptide N-Glycosidase F Treatment

Membrane pellets were resuspended in 1% SDS, 1% β-mercaptoethanol, 35 mM EDTA, and heated to 95°C for 3 min. 10 vol of incubation buffer (50 mM potassium phosphate buffer, pH 6.8, 35 mM EDTA, 1% β-mercaptoethanol, 0.55% octyl glucoside) was added, followed by a second incubation at 95°C for 3 min. Protease inhibitors (1 mM phenylmethylsulfonyl fluoride, 1 mM benzamidine, 20 μg/ml antipain, 1 μg/ml leupeptin, and 1 μg/ml pepstatin) were added, and the reaction mixture was divided into two parts. PNGase was added to one aliquot, and both reaction mixtures were incubated at 37°C for 12 to 16 h.

Hydrogen Fluoride Treatment

O- and N-linked sugars were removed by anhydrous hydrogen fluoride (HF) cleavage (Mort and Lamport, 1977). Membrane fractions (50 μg protein) were lyophilized and dried in a desiccator containing solid P_2O_5. 250 μl HF was added and samples were treated for 80 min at 0°C. HF was subsequently removed by evaporation in a nitrogen stream.

Tunicamycin Treatment

Yeast cells were grown overnight to early log phase, harvested, resuspended in fresh medium, and grown for 30 min at 30°C. Tunicamycin (10 μg/ml) was added, cells were incubated at 30°C for 60 min, and then subjected to membrane extraction as described in Membrane Extracts and Western Blot Analysis.

Microscopy

To observe the autofluorescence of a fusion protein containing Axl2/Bud10p and green fluorescent protein (GFP), cells in log phase were mounted on 0.5% agarose pads under coverslips sealed with pink or red nail polish. To observe bud scars, cells were stained with calcofluor as described by Pringle (1991). Cells were visualized using a Zeiss Axioplan microscope with the FITC filter set and photographed with a three-chip cooled CCD camera.

Results

Use of the Pseudohyphal Phenotype to Isolate Bud-site Selection Mutants

To identify genes required specifically for the axial budding pattern, we searched for mutants of α cells that exhibited a bipolar, rather than axial, budding pattern. This screening method took advantage of the relationship between pseudohyphal growth and budding pattern. Pseudohyphal growth is exhibited by cells with a bipolar budding pattern, such as **a**/α cells (Gimeno et al., 1992), as well as **a** *bud4* and α *bud4* mutants in the Σ1278b strain background (Sanders and Herskowitz, 1996). In contrast, cells that bud in the axial pattern, such as α strain SY77 (α *ura3-52 hmr**a***::*URA3*), do not exhibit pseudohyphal growth. We screened ~70,000 colonies derived from UV-irradiated SY77 cells for the pseudohyphal growth phenotype. Budding patterns of the 107 mutants that displayed the pseudohyphal phenotype were assayed using a microcolony assay (see Materials and Methods). Ten *BAD* mutants exhibited bipolar budding patterns upon retesting and were shown to be defective in single genes by segregation analysis (see Materials and Methods). Of these, four were de-

fective in *BUD4*, one was defective in *BUD3*, and one in *AXL1* (Chant and Herskowitz, 1991; Fujita et al., 1994). Complementation tests revealed that the four remaining mutants, *bad15*, *bad43*, *bad54*, and *bad85*, defined three additional complementation groups. We show here that the complementation group identified by *bad15* and *bad43* corresponds to the previously identified gene *PMT4*.

bad15 Mutants Have a Daughter-specific Defect in Bud-site Selection

bad15 mutant cells exhibited a novel budding pattern that is neither axial nor bipolar (Table III, line 3). In the axial pattern, cells bud adjacent to the previous division site (Chant and Pringle, 1995; Table III, lines 1 and 7). In the bipolar pattern, daughter cells typically bud distal to the previous division site, whereas mother cells bud either near the division site or distal to the previous division site (Chant and Pringle, 1995; Table III, lines 2 and 6). *bad15* mutants (and to a lesser extent, *bad43* mutants) exhibited a distinctive, unipolar budding pattern in which daughter cells budded distal to the division site, as in the bipolar pattern, and mother cells exhibited a typical axial pattern, budding adjacent to the previous division site (Table III, lines 3 and 5). The similar phenotypes of *bad15* and *bad43* mutants suggested that they might be defective in the same gene. Indeed, these mutants failed to complement (Table III, line 9). To determine whether the *bad15* mutation affected bipolar budding, **a**/α *bad15/bad15* diploids were constructed and analyzed. These strains exhibited normal bipolar budding (Table III, compare lines 2 and 4). These data indicated that the *bad15* mutation affected only the axial budding pattern and primarily the behavior of daughter cells. This conclusion was supported by observing the budding patterns of *bad15* cells over several generations. In one experiment in which eleven separate pedigrees were followed, 38/39 *bad15* mother cells budded towards the previous division site, whereas 27/28 *bad15* daughter cells budded away from the previous division site. Nine daughter cells in this experiment divided to become mother cells that divided again. In all cases, these cells budded towards the previous division site in the next cell cycle when they became mothers. These data demonstrated that the *bad15* budding defect was exhibited only by daughter cells and not by mother cells.

Table III. Mutants Defective in bad15 Display a Daughter-specific Defect in Bud-site Selection

Relevant genotype	% Class I	% Class II	% Class III	% Class IV Other	*n*
1. α *BAD15*	98	1	<1	<1	200
2. ***a***/α *BAD15/BAD15*	7	33	53	7	600
3. α *bad15*	21	71	5	4	300
4. ***a***/α *bad15/bad15*	9	20	63	8	300
5. α *bad43*	22	51	21	6	100
6. α *bud4*	10	27	40	24	300

Relevant genotype	% Class I	% Classes II, III, IV	*n*
7. ***a1***$^-$/α *bad15/+*	93	7	100
8. ***a1***$^-$/α *bad15/bad15*	15	85	100
9. ***a1***$^-$/α *bad43/bad15*	12	88	100

Budding pattern was determined by analyzing the morphology of microcolonies (see Materials and Methods). Class I, axial pattern, mother and daughter cells budded adjacent to the previous division site; Class II, mother cells budded near the previous division site, daughter cells budded distal to the previous division site; Class III, both mother and daughter cells budded distal to the previous division site; Class IV, all other microcolony morphologies. Class II and III together represent the bipolar budding pattern. The mother cell is drawn on the left. Strains used were: SY77, line 1; SY204, line 2; SY167, line 3; SY202, line 4; SY172, line 5; SY171, line 6; SY221 × IH2531, line 7; SY221 × SY167, line 8; and SY221 × SY172, line 9.

To determine whether *bad15* mother cells exhibited normal axial budding, bud scars were analyzed by calcofluor staining. Since *bad15* is an allele of *PMT4* (see below), a complete deletion of *PMT4* was used for this study. Cells with a single bud or bud scar and a visible birth scar were scored. Consistent with the microcolony data, which suggest that daughter cells budded incorrectly, only 29% of *pmt4* cells placed the first bud or bud scar adjacent to the birth scar. Rather, 66% of *pmt4* cells placed the first bud or bud scar opposite the birth scar (n = 100), as is typical of the first bud in the bipolar pattern (Chant and Pringle, 1995). In contrast, 94% of wild-type (WT) cells positioned a bud or bud scar adjacent to the birth scar (n = 100), as is typical of the axial budding pattern (Chant and Pringle, 1995). However, after the initial incorrect bud-site selection event, *pmt4* mother cells budded in an axial pattern (Fig. 1, top, compare *PMT4* to *pmt4*::*LEU2*). 99% of the bud scars in both WT and *pmt4* cells with two bud scars or a bud and a bud scar were adjacent (n = 100 in both cases), as is typical of the axial budding pattern (Chant and Pringle, 1995). In addition, 96% of the bud scars in WT and 92% of the bud scars in *pmt4* cells with three or more scars were adjacent (n = 300). The calcofluor staining pattern of WT and *pmt4* cells with three or more bud scars was indistinguishable, suggesting that *pmt4* cells bud axially after an initial incorrect bud-site selection choice.

bad15 Mutants Are Defective in the PMT4 Gene

The *BAD15* gene was cloned by screening for reversal of the pseudohyphal behavior of *bad15* strain SY167. Only subclones containing the *PMT4* gene were able to complement the bud-site selection defect of *bad15* mutants (Fig. 2; Table IV, lines 1–4). Pmt4p is one of seven yeast enzymes that initiate addition of O-linked oligosaccharides to proteins (Gentzsch and Tanner, 1996). *BAD15* was confirmed to be allelic to *PMT4* from the following experiments. First, *pmt4* mutants failed to complement the bud-site selection defect of *bad15* mutants, although both *pmt4* and *bad15* mutations were recessive (Table IV, lines 5, 6 and 7). Second, the same spectrum of proteins underglycosylated in *pmt4* mutants was underglycosylated in *bad15* and *bad43* mutants (data not shown). Third, the bud-site selection phenotype of strains with mutations in *PMT4* was identical to that of *bad15* and *bad43* mutants: all exhibited an axial budding defect that was daughter-specific, resulting in unipolar, rather than axial or bipolar budding (Table V, lines 8–13). Fourth, *BAD15* and *PMT4* exhibited tight genetic linkage: only two axial-budding recombinants were found in 13 tetrads (52 segregants) in crosses between α *bad15* (SY167) and ***a*** *pmt4*::*LEU2* (SY450).

The seven yeast pmt enzymes have different substrate specificities: for example, O-glycosylation of Bar1p and Cts1p is severely affected by mutations in *PMT1* and

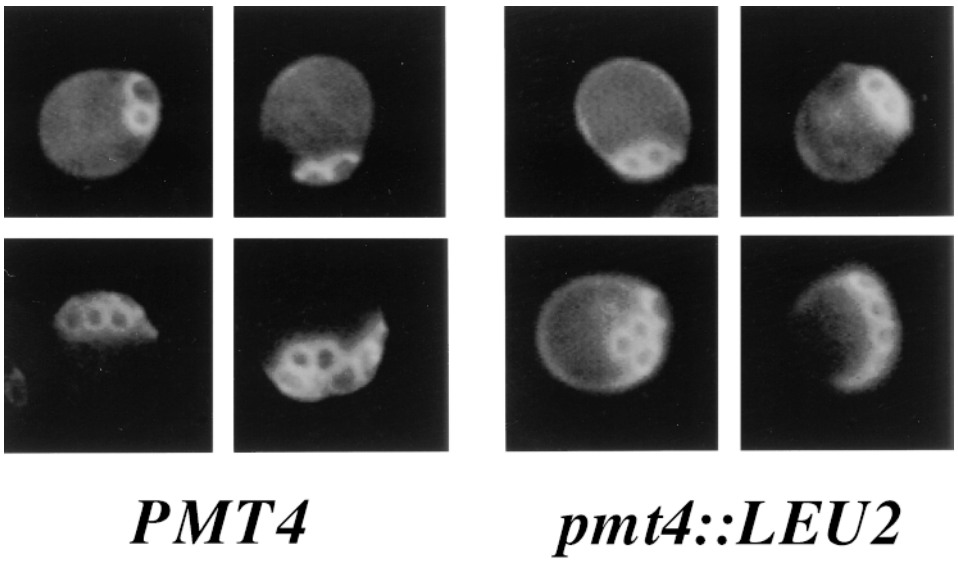

Figure 1. bad15/pmt4 mother cells bud in an axial pattern. WT cells (IH1783, *PMT4*) or cells lacking the *BAD15/PMT4* gene (SY450, *pmt4*::*LEU2*) were stained with calcofluor. Cells with two bud scars (top) or ≥3 bud scars (bottom) were counted and photographed.

PMT2, but not by mutations in *PMT4*. In contrast, O-glycosylation of Kex2p and Gas1p/Gpg1p/gp115 is severely affected by mutations in *PMT4*, but not by mutations in *PMT1* and *PMT2* (Gentzsch and Tanner, 1996, 1997). To determine if *PMT4* is unique among *PMT* genes in being required for normal budding pattern, mutants defective in each of the *PMT* genes were analyzed. Of the six *pmt* mutants tested, only *pmt4* mutants exhibited altered budding patterns (Table V, lines 1–7). The difference in penetrance of the *pmt4* phenotype in the experiments shown in Tables III and V was due to differences in the strain backgrounds (data not shown).

Pmt4p Promotes Addition of O-linked Oligosaccharides to Axl2/Bud10p

Since Pmt4p is a protein mannosyl transferase, we hypothesized that it was involved in O-glycosylation of a protein required for axial budding. Because PMT activity is confined to the ER, only proteins that pass through the ER can be glycosylated by these enzymes. Of all the proteins known to be involved in axial bud-site selection, only Axl2/Bud10p transits the secretory pathway (Roemer et al., 1996) and thus, is a candidate for O-glycosylation. We have used an epitope-tagged allele, *AXL2/BUD10-HA*, which complements *axl2/bud10* mutations (Roemer et al., 1996), to test whether Axl2/Bud10p is a substrate for Pmt4p.

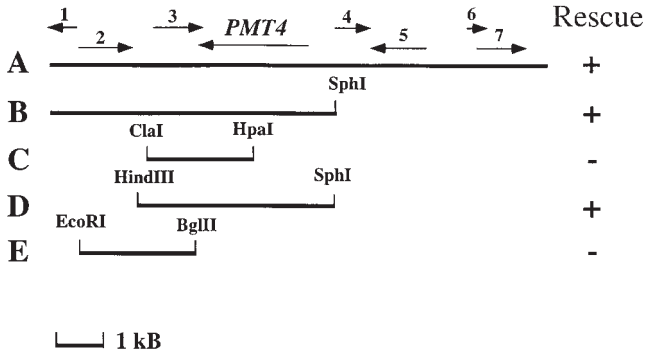

Figure 2. The budding pattern defect of the *bad15* mutant is complemented by plasmids containing *PMT4*. SY167 cells (α *bad15*) were transformed with the indicated plasmids. A, B7; B, pSS44; C, pSS45; D, pSS47; E, pSS46. Black lines indicate DNA present in the clones. Arrows indicate the direction of transcription of individual ORFs. 1, YJR140C; 2, YJR141W; 3, YJR142W; 4, YJR144W; 5, YJR145C; 6, YJR146W; 7, YJR147W. Budding pattern of the transformants was scored using a microcolony assay (Materials and Methods).

Because a lack of O-linked sugars might cause a change in the apparent molecular weight of Axl2/Bud10p, its mobility in *pmt* mutants was examined by SDS-PAGE (Fig. 3). Full-length Axl2/Bud10p (~205 kD) was found in all *pmt* mutants, with the exception of *pmt4* (Fig. 3 A), in which smaller fragments (~43–59 kD) accumulated. Since the predicted molecular weight of the Axl2/Bud10p ORF is ~91 kD, these data indicated that Axl2/Bud10p had undergone proteolytic cleavage. These 43–59-kD fragments, found exclusively in the membrane fraction (M. Gentzsch and W. Tanner, unpublished data), apparently lacked N-linked oligosaccharides, as their mobility did not change after treatment with PNGase (Fig. 3 B).

Fortuitously, studies of Axl2/Bud10p in the presence of tunicamycin revealed a stabilized form of the protein in *pmt4* cells (Fig. 4 A). We do not understand the nature of this tunicamycin-induced stabilization. In the presence of

Table IV. bad15 Mutants Are Defective in PMT4 Activity

Relevant genotype	Plasmid	% Class I	% Classes II, III, IV	*n*
1. *BAD15*	YCp50	80	20	200
2. *BAD15*	*PMT4*	79	21	100
3. *bad15*	YCp50	7	93	171
4. *bad15*	*PMT4*	76	24	301
5. *mat*::*URA3*/α *pmt4*::*LEU2/bad15*	none	25	75	300
6. ***a1***$^{-}$/α *bad15/BAD15*	none	92	8	300
7. *mat*::*URA3*/α *pmt4*::*LEU2/PMT4*	none	97	3	300

Budding pattern was determined by analyzing the morphology of microcolonies as described in the legend to Table III (see also Materials and Methods). Strains used were: IH2531, lines 1 and 2; SY167, lines 3 and 4; SY748 × SY167, line 5; IH1785 × SY167, line 6; and SY748 × SY96, line 7.

Table V. Mutants Defective in PMT4, but Not other PMT Genes, Have Altered Budding Patterns

Relevant genotype	% Class I	% Class II	% Classes III & IV	n
1. Pmt$^+$	93	7	<1	200
2. *pmt1*	90	5	5	200
3. *pmt2*	97	2	1	200
4. *pmt3*	91	6	3	200
5. *pmt4*	59	38	3	200
6. *pmt5*	92	6	2	200
7. *pmt6*	90	8	2	116
8. ***a*** Pmt$^+$	96	2	2	200
9. ***a*** *pmt4*::*LEU2*	5	86	9	200
10. α Pmt$^+$	96	3	1	155
11. α *pmt4*::*LEU2*	13	77	10	179
12. ***a***/α Pmt$^+$	16	27	57	200
13. ***a***/α *pmt4*::*LEU2*/*pmt4*::*LEU2*	1	43	56	600

Budding pattern was determined by analyzing the morphology of microcolonies as described in the legend to Table III (see also Materials and Methods). Strains used were: SY414, line 1; SY655, line 2; SY656, line 3; SY657, line 4; SY415, line 5; SY658, line 6; SY659, line 7; MY13, line 8; SY447, line 9; MY16, line 10; SY448, line 11; SY463, line 12; and SY464, line 13.

tunicamycin, Axl2/Bud10p from WT cells migrated at ~125 kD. The absence of fully glycosylated (~205 kD) Axl2/Bud10p suggests that its half-life is short since all is cleared within the 60 min tunicamycin treatment. Axl2/Bud10p from *pmt4* mutants migrated at ~114 kD under the same conditions, indicating that Axl2/Bud10p in *pmt4* mutants lacked a posttranslational modification. The modification was characterized by subjecting the Axl2/Bud10p species from tunicamycin-treated WT and *pmt4* cells to treatment with HF to release remaining carbohydrates (O-linked sugars; Fig. 4 B). HF treatment of WT extracts resulted in a further reduction in molecular weight of Axl2/Bud10p to ~100 kD, indicating that it is an O-glycosylated protein (Fig. 4 B, compare WT + HF to WT-HF). After treatment with HF, Axl2/Bud10p from *pmt4* cells comigrated with the Axl2/Bud10p from WT cells at ~100 kD (Fig. 4 B, compare + HF samples). The shift in SDS-PAGE mobility of the 114-kD form of Axl2/Bud10p from *pmt4* mutants indicated that it possessed some O-linked

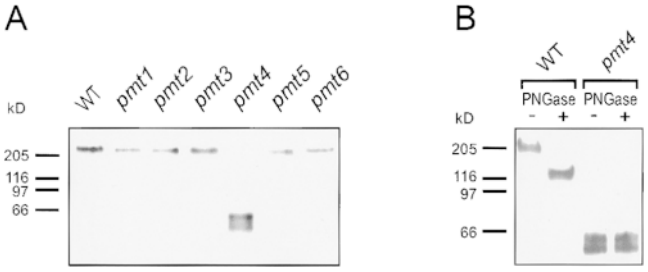

Figure 3. Axl2/Bud10p in *pmt4* mutants is degraded, membrane-associated, and lacks N-linked sugars. (A) Membrane extracts were prepared from WT (MGY60) and *pmt* mutant cells (MGY61-66) producing AXL2-HA (Material and Methods). Extracts were separated by SDS-PAGE and visualized by immunoblotting using anti-HA antibodies. (B) Extracts from WT (MGY60) and a *pmt4* mutant (MGY64) were treated with PNGase. Samples were separated by SDS-PAGE and visualized by immunoblotting.

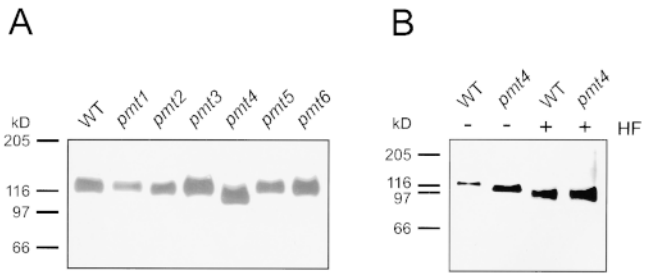

Figure 4. Axl2/Bud10p is stabilized in *pmt4* cells treated with tunicamycin and is incompletely O-glycosylated. (A) WT (MGY60) and *pmt* mutant cells (MGY61-66) were treated with tunicamycin (Materials and Methods). Membrane extracts were prepared, separated by SDS-PAGE, and visualized by immunoblotting. (B) Membranes of tunicamycin-treated WT (MGY60) and *pmt4* cells (MGY64) were subjected to further deglycosylation by treatment with HF. Samples were separated by SDS-PAGE and visualized by immunoblotting.

oligosaccharide (Fig. 4 B, compare *pmt4* samples). These observations indicate that Axl2/Bud10p from *pmt4* mutants and from WT cells both contained O-linked oligosaccharides, but that Axl2/Bud10p received fewer O-linked oligosaccharides in *pmt4* cells than in WT cells. Axl2/Bud10p received ~25 kD of O-linked oligosaccharides: ~13 kD are Pmt4p-independent; the remainder are Pmt4p-dependent.

In contrast to its behavior in *pmt4* strains, Axl2/Bud10p from tunicamycin-treated *pmt1*, *pmt2*, *pmt3*, *pmt5*, and *pmt6* strains was almost indistinguishable in size from WT Axl2/Bud10p (Fig. 4 A). Longer SDS-PAGE runs, which separated proteins of high molecular weight, showed that Axl2/Bud 10p was slightly smaller in *pmt1* and *pmt2* strains (data not shown). Addition of the Pmt4p-independent O-linked oligosaccharides present on Axl2/Bud10p in *pmt4* mutants may be added by Pmt1p and Pmt2p.

Degradation of Axl2/Bud10p Probably Occurs in the Golgi Apparatus

To determine the subcellular compartment in which proteolysis of Axl2/Bud10p occurred in *pmt4* cells, Axl2/Bud10p was analyzed in strains with temperature-sensitive mutations in *sec18* and *sec7*, which disrupt secretory traffic from the ER to the Golgi apparatus and through the Golgi apparatus, respectively (Novick et al., 1981). Axl2/Bud10p was degraded in *pmt4 sec18* cells grown at permissive temperature (Fig. 5, left, 25°C). Incubation of cells at 37°C resulted in accumulation of full-length, nondegraded Axl2/Bud10p (Fig. 5, left, 37°C). In contrast, Axl2/Bud10p was degraded at both 25°C and 37°C in the *sec7 pmt4* strain (Fig. 5, right). These data suggested that degradation of Axl2/Bud10p occurred after the secretory block imposed by *sec18* and before the block imposed by *sec7*. Thus, degradation of Axl2/Bud10p most likely occurred in the Golgi apparatus.

If Axl2/Bud10p is degraded in the Golgi apparatus, its cleavage should be independent of vacuolar proteases. That prediction was borne out. Mutations in the genes encoding vacuolar proteases Pep4p, Prb1p, and Prc1p did not prevent degradation of full-length Axl2/Bud10p in

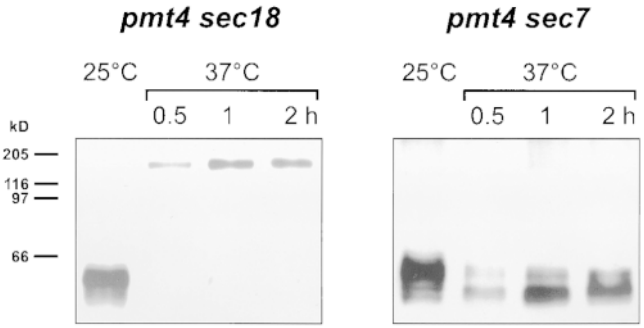

Figure 5. Degradation of Axl2/Bud10p in *pmt4* mutants occurs in the Golgi apparatus. Mutant strains, *pmt4 sec18* (MGY78) and *pmt4 sec7* (MGY76), were grown at the permissive temperature (25°C) or at 37°C to induce the secretory block. Membrane extracts were prepared, separated by SDS-PAGE, and visualized by immunoblotting.

pmt4 mutants (Fig. 6 A). Considerably more of the 43–59-kD Axl2/Bud10p species was found in *pmt4 pep4 prb1* and *pmt4 pep4 prb1 prc1* mutants than in *pmt4* mutants alone, suggesting that vacuolar proteases further degrade the 43–59-kD fragments. Degradation of Axl2/Bud10p in *pmt4* mutants was unaffected by mutation of *UBC7*, which encodes a ubiquitin-conjugating enzyme that participates in degradation of ER proteins (Biederer et al., 1997), again suggesting that the cleavage of Axl2/Bud10p does not occur in the ER (Fig. 6 B).

Axl2/Bud10p Is Improperly Localized in pmt4 Mutants

Localization of Axl2/Bud10p is dependent upon cell cycle stage (Halme et al., 1996; Roemer et al., 1996). In early G1 cells, Axl2/Bud10p is found in a patch at the presumptive bud site; it is later found at the periphery of the bud. By the time of the G2/M transition, Axl2/Bud10p is observed on the bud side of the mother-bud neck and is subsequently found on both sides of the mother-bud neck. Axl2/Bud10p persists at the neck region of mother and daughter cells past cytokinesis. We made similar observations in our

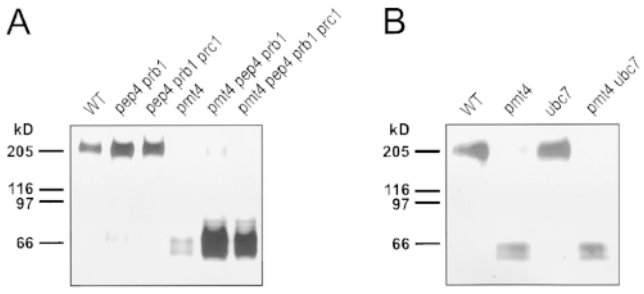

Figure 6. Initial cleavage of Axl2/Bud10p in *pmt4* mutants does not depend on vacuolar proteases or the ER-linked proteolytic system. (A) Membrane extracts were prepared, separated by SDS-PAGE, and visualized by immunoblotting from *PMT4* or *pmt4* cells possessing (MGY69 or MGY72) or lacking (MGY70, 71, 73, 74) vacuolar proteases Pep4, Prb1p, and Prc1p. (B) Membrane extracts were prepared, separated by SDS-PAGE, and visualized by immunoblotting from *PMT4* or *pmt4* cells possessing (MGY69 or MGY72) or lacking (MGY67 or 68) ubiquitin conjugating enzyme Ubc7p.

Pmt^+ strain background using cells that produce a fusion of Axl2/Bud10p to the GFP (Halme et al., 1996; Fig. 7, a–f). 97% of fluorescent WT cells in an asynchronous population exhibited strong staining that fell into one of three classes. Almost 50% of cells (202/407) exhibited staining at bud periphery (Fig. 7, a and b). 30% of cells (121/407) exhibited staining predominantly at the bud side of the mother-bud neck (Fig. 7, c and d). 17% exhibited strong staining that was symmetrically distributed with respect to the mother-bud neck (Fig. 7, e and f). Though we detected no difference in the distribution of cells with respect to the cell cycle in *pmt4* mutants versus WT cells, only 10% of *pmt4* cells (37/369) exhibited staining that fell into the three classes defined by WT cells. Most mutant cells exhibited a strikingly different localization pattern (Fig. 7, g–l): 58% (216/369) exhibited a punctate intracellular pattern (Fig. 7, g, h, i, k, and l) that resembled the Golgi apparatus (Franzusoff et al., 1991; Redding et al., 1991). Such staining was seen in only 3% of Pmt^+ cells. 13% of *pmt4* cells with these punctate intracellular patches also exhibited relatively normal staining at the bud periphery (28/216; Fig. 7, g [right cell] and h). Many *pmt4* cells (206/369) accumulated Axl2/Bud10p at the neck. However, unlike WT cells, the neck staining was enriched on, or was specific to, the mother side of the mother-bud neck (78/369 cells; Fig. 7, i and j) or faint, but equally distributed on either side of the neck (121/369 cells; Fig. 7, k and l). None of the neck staining in WT cells was observed in either of these two categories. Localization of the Bud4 protein was unaffected by mutation of *pmt4* (data not shown).

Overexpression of AXL2/BUD10 Partially Restores Axial Bud-site Selection to pmt4 Mutants

If Axl2/Bud10p activity is decreased due to the lack of O-linked oligosaccharides, overexpression of *AXL2/BUD10* might partially restore the axial budding pattern to *pmt4* mutants. To test this possibility, *pmt4* and WT strains were transformed with YEp24-*AXL2*, which carries *AXL2/BUD10* on a high copy plasmid. This plasmid slightly decreased the axial budding of WT cells, from 93 to 76% axial. In contrast, YEp24-*AXL2* partially rescued the unipolar budding pattern of *pmt4* mutants to axial, increasing axial budding from 5 to 40%.

Discussion

Axl2/Bud10p is a transmembrane glycoprotein required for yeast cells to exhibit the axial budding pattern (Halme et al., 1996; Roemer et al., 1996). Like Bud3p and Bud4p (Chant et al., 1995; Sanders and Herskowitz, 1996), it is proposed to function as an intracellular landmark: Axl2/Bud10p localizes to both sides of the mother-bud neck for part of the cell cycle and is inherited by both mother and daughter cells at the position of bud emergence in the previous cell cycle. Through the isolation and characterization of mutants with altered bud-site selection, we have uncovered a requirement for O-linked glycosylation by the mannosyl transferase Pmt4p, which presumably acts directly on Axl2/Bud10p. Though O-linked glycosylation has been assumed to be important for protein function, identifying specific roles for this modification on particular pro-

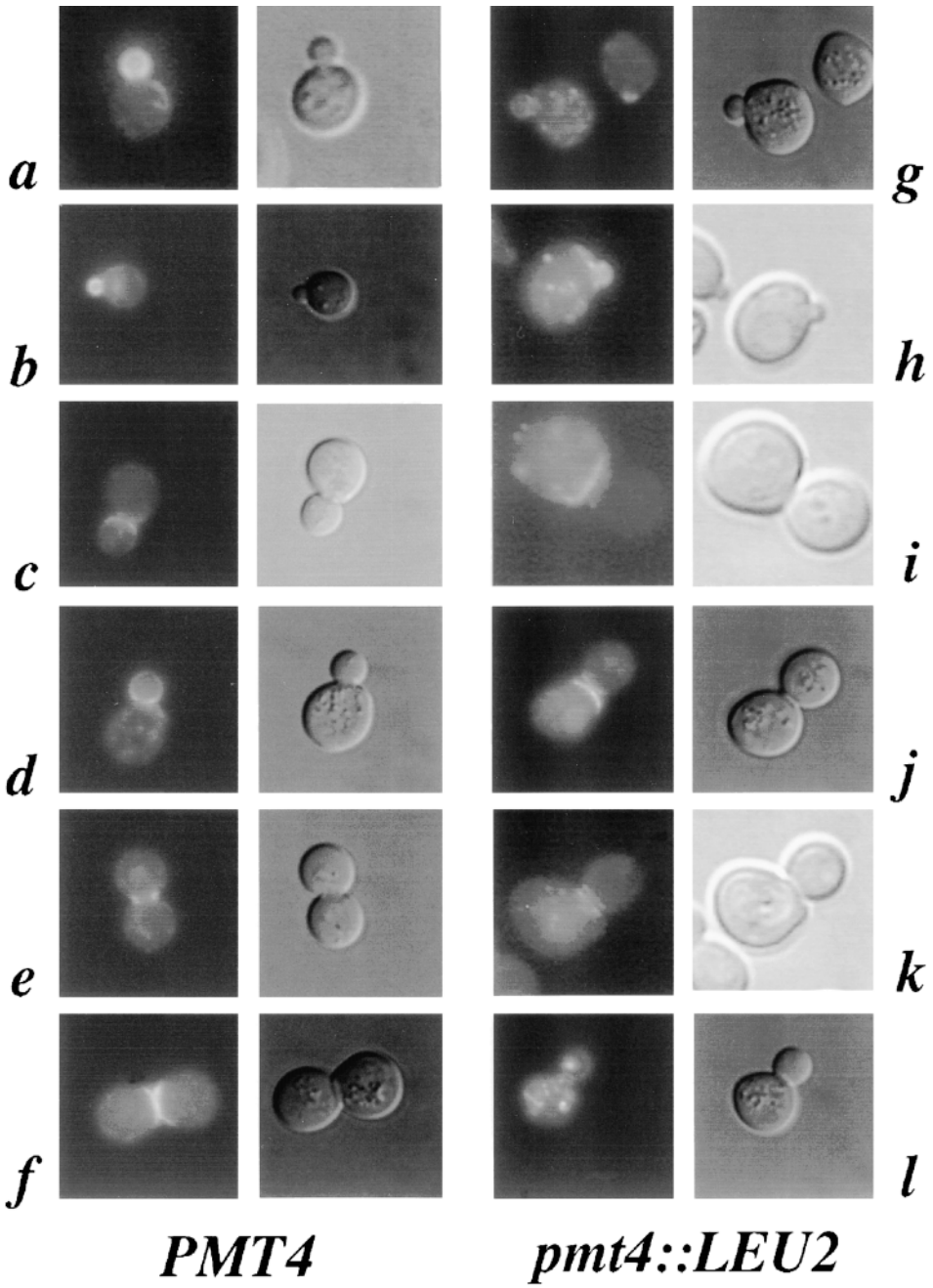

Figure 7. Axl2/Bud10p is improperly localized in *pmt4* mutants. IH1783 cells (*PMT4*, a–f) or SY450 cells (*pmt4*::*LEU2*, g–l) carried pAH14, a low-copy plasmid encoding Axl2/Bud10p-GFP. Cells were grown to early log phase, sonicated, and visualized by fluorescence microscopy.

teins has been elusive. We suggest that O-linked glycosylation of Axl2/Bud10p promotes its movement through the secretory pathway, prevents its degradation, and allows Axl2/Bud10p to function on the cell surface to assemble components required for bud emergence.

O-linked Glycosylation by Pmt4p Enhances the Stability of Axl2/Bud10p

Axl2/Bud10p acquires O-linked oligosaccharides, some of which are dependent upon Pmt4p. Only the Pmt4p-dependent sugars appear to be important for Axl2/Bud10p function. Because Axl2/Bud10p in *pmt4* mutants contains some O-linked oligosaccharide, it is clear that the simple presence of O-linked oligosaccharide is not sufficient to facilitate Axl2/Bud10p protein function. It appears that, as with protein phosphorylation, the amount of O-linked oligosaccharide or the specific sites of modification are important for function. Studies of Axl2/Bud10p provide an opportunity to identify the determinants for recognition by Pmt4p and other PMT proteins. Because proteins, such as Kex2p and Gas1p/gp115/Ggp1p are glycosylated primarily by Pmt4p (Gentzsch and Tanner, 1997), comparison of Kex2p, Gas1p/gp115/Ggp1p, and Axl2/Bud10p may help to identify consensus acceptor sequences for Pmt4p-dependent O-linked glycosylation. All three proteins have extracellular domains rich in serine and threonine residues that are close to the membrane (Mizuno et al., 1988; Vai et al., 1991; Halme et al., 1996; Roemer et al., 1996). These do-

mains are glycosylated in the case of Kex2p and Gas1p/gp115/Ggp1p (Fuller et al., 1989; Wilcox and Fuller, 1991; Gatti et al., 1994; Gentzsch and Tanner, 1997), and perhaps Axl2/Bud10p as well. Serine- and threonine-rich domains close to the membrane may be recognized specifically by Pmt4p.

Pmt4p is required for the stability of Axl2/Bud10p. Axl2/Bud10p is a large, type I integral protein of the plasma membrane. In *pmt4* mutants, Axl2/Bud10p is cleaved to produce stable membrane-associated fragments of ~43–59 kD, which appear to be the cytoplasmic-transmembrane segment of Axl2/Bud10p. This structure is inferred from three lines of evidence. First, the fragments are recognized by antibodies specific for an epitope tag at the COOH terminus of Axl2/Bud10p. Second, as these fragments are membrane-associated, they presumably also contain the transmembrane domain. Third, these fragments lack both N- and O-linked oligosaccharides, which should be present solely in the extracellular domain. Roemer et al. (1996) determined that Axl2/Bud1p is a type I membrane protein by demonstrating that the COOH terminus of Axl2/Bud10p is refractory to degradation by proteases added extracellularly. The apparent molecular weight of the protease-resistant fragments (a collection of fragments 50–55 kD) is similar to that of the fragments we observe in *pmt4* mutants (43–59 kD), adding further credence to the notion that the fragments contain the COOH terminus of Axl2/Bud10p joined to the transmembrane domain. We do not know the fate of the remaining ~40% of Axl2/Bud10p, which includes the NH_2-terminal segment.

Two lines of evidence suggest that the initial degradation of Axl2/Bud10p in *pmt4* mutants occurs in the Golgi apparatus. First, proteolytic cleavage of Axl2/Bud10p occurs in *sec7 pmt4*, but not in *sec18 pmt4* mutants, suggesting that cleavage requires transit to the Golgi apparatus and occurs even when further transport is inhibited. Consistent with this notion, cleavage of Axl2/Bud10p to the ~55-kD fragments does not require vacuolar proteases. The accumulation of these ~55-kD fragments in *pep4 prb1* and *pep4 prb1 prc1* cells suggested that once generated, these fragments are degraded in the vacuole.

Previous studies have revealed an effect of O-glycosylation on protein stability. Axl2/Bud10p is stabilized in *pmt4* mutants grown in the presence of the N-linked glycosylation inhibitor, tunicamycin. We do not know the reason for this stabilization. One possibility is that in the absence of N-linked sugars, Axl2/Bud10p cannot reach the Golgi apparatus, where its initial degradation occurs. However, Axl2/Bud10p localization in *pmt4* mutants appears the same in the presence versus absence of tunicamycin (data not shown). We favor a second possibility, that the conformation of Axl2/Bud10p lacking its N-linked sugars makes it a poorer substrate for proteolytic degradation. Several proteins, including the low density lipoprotein (LDL) receptor, decay accelerating factor, major envelope protein of Epstein-Barr virus, Kex2p, and neurotrophin receptor are less stable when they lack O-linked oligosaccharides (Kozarsky et al., 1988; Fuller et al., 1989; Reddy et al., 1989; Monlauzeur et al., 1998). Not all O-linked oligosaccharides are important for protein function, however: Gas1p/Ggp1p/gp115 and human chorionic gonadotropin lacking O-linked oligosaccharides (Matzuk et al., 1987; Gatti et al., 1994) are indistinguishable in stability from their glycosylated counterparts.

Instability of Axl2/Bud10p and its failure to accumulate efficiently at the cell surface without modification by Pmt4p are probably coupled, though it is unclear which is the primary consequence of the O-glycosylation defect. Perhaps unmodified Axl2/Bud10p is recognized as a misfolded protein and targeted for destruction by a quality control system of the Golgi apparatus. Resulting proteolytic fragments might be inefficiently targeted to the plasma membrane. Another possibility is that absence of Pmt4p-dependent modifications delays movement of Axl2/Bud10p through the secretory pathway, increasing the probability of cleavage by a resident Golgi protease. Some Axl2/Bud10p does assemble at the bud periphery and neck in *pmt4* cells, though the amount is reduced with respect to WT cells. As for the LDL receptor (Kozarsky et al., 1988), the lack of O-linked oligosaccharide may also affect Axl2/Bud10p stability once it reaches the plasma membrane. Axl2/Bud10p seems to be inherently unstable.

PMT4 Is Required for Proper Budding Only in Daughter Cells

Because cells defective in *PMT4* exhibit a bud-site selection defect, we initially predicted the existence of a Pmt4p substrate protein important for accurate budding. Our studies indicate that Axl2/Bud10p is the Pmt4p substrate relevant to bud-site selection: Axl2/Bud10p is O-glycosylated, unstable and mislocalized in *pmt4* mutants, and its overproduction can partially rescue the *pmt4* phenotype. The requirement for Pmt4p only in daughter cells might be explained in a variety of ways. In principle, Axl2/Bud10p might be required only in daughter cells, or its glycosylation might be necessary only in daughter cells. Because Axl2/Bud10p is required for bud-site selection in both mother and daughter cells (Halme et al., 1996; Roemer et al., 1996), the first explanation appears to be incorrect. Therefore, we entertain a second possibility, that O-linked glycosylation of Axl2/Bud10p by Pmt4p is required only in daughter cells. Perhaps O-glycosylation is not needed to stabilize Axl2/Bud10p in mother cells. This explanation is unlikely, since a single, partially degraded population of Axl2/Bud10p is detected by Western blot (Fig. 3 A), and intracellular patches of Axl2/Bud10p accumulate in both mother and daughter cells (Fig. 7). Another possibility is that mother cells can accommodate the reduction of Axl2/Bud10p activity in *pmt4* mutants, whereas daughter cells cannot. We favor this third possibility.

The differences between mother and daughter cells in the requirement for *PMT4* may arise from differences in the path by which Axl2/Bud10p reaches the mother-bud neck (Fig. 8). Axl2/Bud10p is thought to become localized to the bud side of the mother-bud neck by reorganization of protein in cells with a small bud (Fig. 8 A, 2 and 3). Localization of Axl2/Bud10p at the mother side of the mother-bud neck is hypothesized to occur subsequently by new synthesis within the mother cell (Roemer et al., 1996; Fig. 8 A, 3). After cytokinesis, both mother and daughter cells inherit a patch of Axl2/Bud10p, which promotes utilization of axial bud sites. In *pmt4* mutants, we propose that

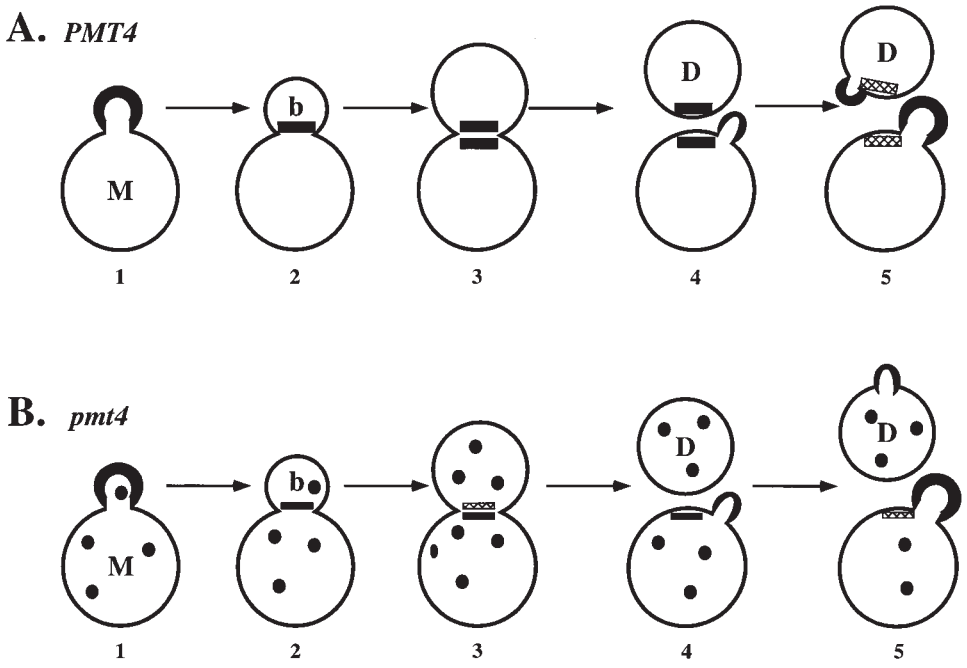

Figure 8. The daughter cell-specific budding pattern phenotype of *pmt4* mutants may be explained by reduced activity of Axl2/Bud10p in both mother and daughter cells. (A) WT cells. 1, Axl2/Bud10p (black crescent) is localized at the periphery of a WT bud. 2, Axl2/Bud10p is reorganized to the bud side of the mother-bud neck. 3, New synthesis of Axl2/Bud10p leads to its accumulation on the mother side of the mother-bud neck. 4, After cytokinesis, both mother and daughter cells inherit a patch of Axl2/Bud10p. The mother cell initiates bud formation adjacent to the residual patch of Axl2/Bud10p. 5, The daughter cell initiates bud formation adjacent to the residual patch of Axl2/Bud10p. The residual patches of Axl2/Bud10p disappear (hatched rectangles). (B) *pmt4* cells: 1, Axl2/Bud10p (black crescent) is localized at the periphery of a *pmt4* mutant bud. Axl2/Bud10p is also found in punctate intracellular patches (black circles). 2, Axl2/Bud10p is reorganized to the bud side of the mother-bud neck. The reduced accumulation of Axl2/Bud10p to the bud neck is represented by the small size of the black rectangle (compare to A 2). 3, New synthesis of Axl2/Bud10p leads to its accumulation on the mother side of the mother-bud neck. The unstable Axl2/Bud10p disappears from the bud side of the mother-bud neck. 4, After cytokinesis, only mother cells inherit a patch of Axl2/Bud10p. The mother cell initiates bud formation adjacent to the residual patch of Axl2/Bud10p. 5, The daughter cell initiates bud formation using bipolar information, since it lacks a residual patch of Axl2/Bud10p. The residual patch of Axl2/Bud10p disappears from the mother cell (hatched rectangles).

Axl2/Bud10p is at a reduced level, so that the activity in the daughter side of the mother-bud neck is inadequate (Fig. 8 B). In contrast, newly synthesized Axl2/Bud10p, which becomes localized to the mother side of the mother-bud neck (Fig. 8 B, 3), is proposed to be adequate for promoting utilization of axial bud sites after cytokinesis (Fig. 8 B, 4). In other words, Axl2-Bud10p used for axial budding in daughter cells must persist from S phase until the next G1 phase, whereas that in mother cells need persist only from late mitosis until the next G1 phase. That daughter cells exhibit a longer G1 phase than do mother cells might also make it harder for Axl2/Bud10p to persist until it is needed again in daughter cells. Support for the proposal that Axl2-Bud10p is differentially affected in mother and daughter cell compartments comes from the observation that Axl2-Bud10p can be observed preferentially on the mother side of the mother-bud neck in a substantial fraction of *pmt4* mutant cells (21%), a distribution that is rare in WT cells (0.25%). For the 33% of *pmt4* cells that exhibited faint Axl2/Bud10p staining on both sides of the mother-bud neck, we argue that this level of Axl2/Bud10p is sufficient for bud-site selection in mother cells, but is inadequate in daughter cells.

Several functional differences between mother and daughter cells have been described previously. Mother cells can switch mating type, whereas daughter cells cannot (Strathern and Herskowitz, 1979); mother cells specifically inherit plasmids containing autonomously replicating sequences (ARS) and lacking centromere sequences, whereas daughter cells do not (Murray and Szostak, 1983); and mother cells budding in the bipolar pattern may bud distal or proximal to the birth site, whereas new daughter cells bud primarily at distal sites (Chant and Pringle, 1995). O-glycosylated cell-surface molecules certainly contribute to selection of bud sites in **a**/α cells: both Bud8p and Bud9p appear to be O-glycosylated (Zahner et al., 1996; N. Pagé, H. Bussey, J.R. Pringle, personal communication). Here, we have observed that the integrity of an O-glycosylated landmark protein can differentially affect the behavior of mother and daughter cells and generate an asymmetric cell division. Asymmetrically located landmarks that are anchored to the cell wall by O-glycosylated proteins might contribute to the asymmetric switching of mating type and plasmid inheritance as well.

We thank David Rivier, Mary Maxon, Carlos Gimeno, Gerry Fink, Merrilyn Mitchelitch, John Chant, Terry Roemer, Mike Snyder, Gunther Daum, Dieter Wolf, and Thomas Sommer for strains and plasmids. We are grateful to Ludwig Lehle for assistance with the HF experiments, Chi Tu for analysis of *bad* mutants, Tom Wang for demonstrating the allelism between *BAD15* and *BAD43*, Ramon Tabtiang for sequencing the ends of the B7 clone, and Aji Kron for assistance in figure preparation. We appreciate discussions with members of the Herskowitz laboratory and Anita Sil, Frank Solomon, Steve Bell, and Ramon Tabtiang for comments on the manuscript.

This work was supported by a postdoctoral fellowship from the Helen Hay Whitney Foundation and a Burroughs Wellcome Career Award in the Biomedical Sciences to S.L. Sanders, a grant from the Deutsche Forschungsgemeinschaft (SFB521) to W. Tanner, and a National Institutes of Health research grant (GM48052) to I. Herskowitz.

Received for publication 2 February 1999 and in revised form 29 April 1999.

References

Adams, A.E.M., and J.R. Pringle. 1984. Localization of actin and tubulin in wild-type and morphogenetic-mutant *Saccharomyces cerevisiae*. *J. Cell Biol.* 98:934–945.

Amberg, D.C., E. Basart, and D. Botstein. 1995. Defining protein interactions with yeast actin in vivo. *Nature Struct. Biol.* 2:28–35.

Amberg, D.C., J.E. Zahner, J.W. Mulholland, J.R. Pringle, and D. Botstein. 1997. Aip3p/Bud6p, a yeast actin-interacting protein that is involved in morphogenesis and the selection of bipolar budding sites. *Mol. Biol. Cell.* 8:729–753.

Ausubel, F.M., R. Brent, R.E. Kingston, D.D. Moore, J.G. Seidman, J.A. Smith, and K. Struhl. 1987. *Current Protocols in Molecular Biology*. Wiley Interscience.

Bender, A., and J.R. Pringle. 1989. Multicopy suppression of the *cdc24* budding defect in yeast by *CDC42* and three newly identified genes included the *ras*-related *RSR1*. *Proc. Natl. Acad. Sci. USA*. 86:9976–9980.

Bender, A., and J.R. Pringle. 1991. Use of a screen for synthetic lethal and multicopy suppressee mutants to identify two new genes involved in morphogenesis in *Saccharomyces cerevisiae*. *Mol. Cell. Biol.* 11:1295–1305.

Biederer, T., C. Volkwein, and T. Sommer. 1997. Role of Cue1p in ubiquitination and degradation at the ER surface. *Science.* 278:1806–1809.

Chant, J., and I. Herskowitz. 1991. Genetic control of bud-site selection in yeast by a set of gene products that comprise a morphogenetic pathway. *Cell.* 65: 1203–1212.

Chant, J., and J.R. Pringle. 1995. Patterns of bud-site selection in the yeast *Saccharomyces cerevisiae*. *J. Cell Biol.* 129:751–765.

Chant, J., K. Corrado, J.R. Pringle, and I. Herskowitz. 1991. Yeast *BUD5*, encoding a putative GDP–GTP exchange factor, is necessary for bud site selection and interacts with bud formation gene *BEM1*. *Cell.* 65:1213–1224.

Chant, J., M. Mischke, E. Mitchell, I. Herskowitz, and J.R. Pringle. 1995. Role of Bud3p in producing the axial budding pattern of yeast. *J. Cell Biol.* 129: 767–778.

Field, C., and R. Schekman. 1980. Localized secretion of acid phosphatase reflects the pattern of cell surface growth in *Saccharomyces cerevisiae*. *J. Cell Biol.* 86:123–128.

Franzusoff, A., K. Redding, J. Crosby, R.S. Fuller, and R. Schekman. 1991. Localization of components involved in protein transport and processing through the yeast Golgi apparatus. *J. Cell Biol.* 112:27–37.

Freifelder, D. 1960. Bud position in *Saccharomyces cerevisiae*. *J. Bacteriol.* 80: 567–568.

Fujita, A., C. Oka, Y. Arikawa, T. Katagai, A. Tonouchi, S. Kuhara, and Y. Misumi. 1994. A yeast gene necessary for bud-site selection encodes a protein similar to insulin-degrading enzymes. *Nature.* 372:567–570.

Fuller, R.S., A. Brake, and J. Thorner. 1989. Yeast prohormone processing enzyme (*KEX2* gene product) is a Ca^{2+}-dependent serine protease. *Proc. Natl. Acad. Sci. USA*. 86:1434–1438.

Gatti, E., L. Popolo, M. Vai, N. Rota, and L. Alberghina. 1994. O-linked oligosaccharides in yeast glycosyl phosphatidylinositol-anchored protein gp115 are clustered in a serine-rich region not essential for its function. *J. Biol. Chem*. 269:19695–19700.

Gentzsch, M., and W. Tanner. 1996. The *PMT* gene family: protein O-glycosylation in *Saccharomyces cerevisiae* is vital. *EMBO (Eur. Mol. Biol. Organ.) J.* 15:5752–5759.

Gentzsch, M., and W. Tanner. 1997. Protein-O-glycosylation in yeast: protein-specific mannosyltransferases. *Glycobiology.* 7:481–486.

Gimeno, C.J., P.O. Ljungdahl, C.A. Styles, and G.R. Fink. 1992. Unipolar cell divisions in the yeast *S. cerevisiae* lead to filamentous growth: regulation by starvation and *RAS*. *Cell.* 68:1077–1090.

Halme, A., M. Michelitch, E.L. Mitchell, and J. Chant. 1996. Bud10p directs axial cell polarization in budding yeast and resembles a transmembrane receptor. *Curr. Biol.* 6:570–579.

Haselbeck, A., and W. Tanner. 1983. O-glycosylation in *Saccharomyces cerevisiae* is initiated at the endoplasmic reticulum. *FEBS Lett.* 158:335–338.

Herscovics, A., and P. Orlean. 1993. Glycoprotein biosynthesis in yeast. *FASEB J.* 7:540–550.

Hicks, J.B., J.N. Strathern, and I. Herskowitz. 1977. Interconversion of yeast mating types. III. Action of the homothallism (*HO*) gene in cells homozygous for the mating type locus. *Genetics.* 85:395–405.

Immervoll, T., M. Gentzsch, and W. Tanner. 1995. *PMT3* and *PMT4*, two new members of the protein-O-mannosyltransferase gene family of *Saccharomyces cerevisiae*. *Yeast.* 11:1345–1351.

Kozarsky, K., D. Kingsley, and M. Krieger. 1988. Use of a mutant cell line to study the kinetics and function of O-linked glycosylation of low density lipoprotein receptors. *Proc. Natl. Acad. Sci. USA*. 85:4335–4339.

Loo, S., P. Laurenson, M. Foss, A. Dillin, and J. Rine. 1995. Roles of *ABF1*, *NPL3*, and *YCL54* in silencing in *Saccharomyces cerevisiae*. *Genetics.* 141: 889–902.

Lussier, M., M. Gentzsch, A.M. Sdicu, H. Bussey, and W. Tanner. 1995. Protein O-glycosylation in yeast. The *PMT2* gene specifies a second protein O-mannosyltransferase that functions in addition to the *PMT1*-encoded activity. *J. Biol. Chem*. 270:2770–2775.

Matzuk, M.M., M. Krieger, C.L. Corless, and I. Boime. 1987. Effects of preventing O-glycosylation on the secretion of human chorionic gonadotropoin in Chinese hamster ovary cells. *Proc. Natl. Acad. Sci. USA*. 84:6354–6358.

Mizuno, K., T. Nakamura, T. Ohshima, S. Tanaka, and H. Matsuo. 1988. Yeast *KEX2* gene encodes an endopeptidase homologous to subtilisin-like serine proteases. *Biochem. Biophys. Res. Commun*. 156:246–254.

Monlauzeur, L., L. Breuza, and A.L. Bivic. 1998. Putative O-glycosylation sites and a membrane anchor are necessary for apical delivery of the human neurotrophin receptor in Caco-2 cells. *J. Biol. Chem*. 273:30263–30270.

Mort, A.J., and D.T. Lamport. 1977. Anhydrous hydrogen fluoride deglycosylates glycoproteins. *Analyt. Biochem*. 82:289–309.

Murray, A.W., and J.W. Szostak. 1983. Pedigree analysis of plasmid segregation in yeast. *Cell.* 34:961–970.

Novick, P., and D. Botstein. 1985. Phenotypic analysis of temperature-sensitive yeast actin mutants. *Cell.* 40:405–416.

Novick, P., S. Ferro, and R. Schekman. 1981. Order of events in the yeast secretory pathway. *Cell.* 25:461–469.

Park, H.-O., E. Bi, J.R. Pringle, and I. Herskowitz. 1997. Two active states of the Ras-related Bud1/Rsr1 protein bind to different effectors to determine yeast cell polarity. *Proc. Natl. Acad. Sci. USA*. 94:4463–4468.

Pringle, J.R. 1991. Staining of bud scars and other cell wall chitin with calcofluor. *Methods Enzymol.* 194:732–735.

Redding, K., C. Holcomb, and R.S. Fuller. 1991. Immunolocalization of Kex2 protease identifies a putative late Golgi compartment in the yeast *Saccharomyces cerevisiae*. *J. Cell Biol.* 113:527–538.

Reddy, P., I. Caras, and M. Krieger. 1989. Effects of O-linked glycosylation on the cell surface expression and stability of decay-accelerating factor, a glycophospholipid-anchored membrane protein. *J. Biol. Chem*. 264:17329–17336.

Roemer, T., K. Madden, J.T. Chang, and M. Snyder. 1996. Selection of axial growth sites in yeast requires Axl2p, a novel plasma membrane glycoprotein. *Genes Dev*. 10:777–793.

Rose, M.D., P. Novick, J.H. Thomas, D. Botstein, and G.R. Fink. 1987. A *Saccharomyces cerevisiae* genomic plasmid bank based on a centromere-containing shuttle vector. *Gene*. 60:237–243.

Rose, M.D., F. Winston, and P. Hieter. 1990. Methods in Yeast Genetics: A Laboratory Course. Cold Spring Harbor Laboratory Press, Cold Spring Harbor, NY.

Rothstein, R.J. 1983. One-step gene disruption in yeast. *Methods Enzymol.* 101: 202–211.

Sambrook, J., E.F. Fritsch, and T. Maniatis. 1989. Molecular Cloning: A Laboratory Manual. Cold Spring Harbor Laboratory Press, Cold Spring Harbor, NY.

Sanders, S.L., and I. Herskowitz. 1996. The Bud4 protein of yeast, required for axial budding, is localized to the mother/BUD neck in a cell cycle-dependent manner. *J. Cell Biol.* 134:413–427.

Sikorski, R.S., P. Hieter. 1989. A system of shuttle vectors and yeast host strains designed for efficient manipulation of DNA in *Saccharomyces cerevisiae*. *Genetics*. 122:19–27.

Sloat, B.F., and J.R. Pringle. 1978. A mutant of yeast defective in cellular morphogenesis. *Science.* 200:1171–1173.

Snyder, M., S. Gehrung, and B.D. Page. 1991. Studies concerning the temporal and genetic control of cell polarity in *Saccharomyces cerevisiae*. *J. Cell Biol.* 114:515–532.

Strahl-Bolsinger, S., and W. Tanner. 1991. Protein O-glycosylation in *Saccharomyces cerevisiae.* Purification and characterization of the dolichyl-phosphate-D-mannose-protein O-D-mannosyltransferase. *Eur. J. Biochem*. 196: 185–190.

Strathern, J.N., and I. Herskowitz. 1979. Asymmetry and directionality in production of new cell types during clonal growth: the switching pattern of homothallic yeast. *Cell.* 17:371–381.

Tanner, W., and L. Lehle. 1987. Protein glycosylation in yeast. *Biochim. Biophys. Acta.* 906:81–99.

Tkacz, J., and J. Lampen. 1973. Surface distribution of invertase on growing *Saccharomyces cerevisiae*. *J. Bacteriol.* 113:1073–1075.

Vai, M., E. Gatti, E. Lacana, L. Popolo, and L. Alberghina. 1991. Isolation and deduced amino acid sequence of the gene encoding gp115, a yeast glycophospholipid-anchored protein containing a serine-rich region. *J. Biol. Chem*. 266:12242–12248.

Valtz, N., and I. Herskowitz. 1996. Pea2 protein of yeast is localized to sites of polarized growth and is required for efficient mating and bipolar budding. *J. Cell Biol.* 135:725–739.

Wilcox, C.A., and R.S. Fuller. 1991. Posttranslational processing of the prohormone-cleaving Kex2 protease in the *Saccharomyces cerevisiae* secretory pathway. *J. Cell Biol.* 115:297–307.

Zahner, J.E., H.A. Harkins, and J.R. Pringle. 1996. Genetic analysis of the bipolar pattern of bud site selection in the yeast *Saccharomyces cerevisiae*. *Mol. Cell Biol.* 16:1857–1870.

Zheng, Y., A. Bender, and R.A. Cerione. 1995. Interactions among proteins involved in bud-site selection and bud-site assembly in *Saccharomyces cerevisiae*. *J. Biol. Chem*. 270:626–630.

Ziman, M., D. Preuss, J. Mulholland, J.M. O'Brien, D. Botstein, and D.I. Johnson. 1993. Subcellular localization of Cdc42p, a *Saccharomyces cerevisiae* GTP-binding protein involved in the control of cell polarity. *Mol. Biol. Cell.* 4:1307–1316.